



Title	Lamellar Tearing of 5083 Aluminum Alloy and Its Welds(Materials, Metallurgy, Weldability)
Author(s)	Enjo, Toshio; Kuroda, Toshio; Shinonaga, Hideyuki
Citation	Transactions of JWRI. 1979, 8(2), p. 231-239
Version Type	VoR
URL	<a href="https://doi.org/10.18910/4280">https://doi.org/10.18910/4280</a>
rights	
Note	

*The University of Osaka Institutional Knowledge Archive : OUKA*

<https://ir.library.osaka-u.ac.jp/>

The University of Osaka

# Lamellar Tearing of 5083 Aluminum Alloy and Its Welds†

Toshio ENJO\*, Toshio KURODA\*\* and Hideyuki SHINONAGA\*\*\*

## Abstract

An investigation has been made into the lamellar tearing of 5083 aluminum alloy and its welds at  $-196^{\circ}\text{C}$  by means of fractography. This alloy has rolling texture structure and highly directional grain boundaries. For the longitudinal direction specimen, laminated fracture with many subcracks occurs. The subcracks occur along the flat grain boundary by rolling process, and the main crack is transgranular fracture independent of  $\beta$  phase precipitation. For the short transverse direction specimen, lamellar tearing occurs, which shows terrace and wall type's fracture.

When  $\beta$  phase hardly precipitates, the fracture morphology shows transgranular fracture, and relatively insoluble compounds and inclusions are present at the bottom of dimple in the terrace area. When  $\beta$  phase precipitates at the grain boundary continuously, the fracture morphology shows intergranular fracture. In the case of non-recrystallization structure, lamellar tearing of terrace and wall type occurs in spite of intergranular fracture. On the implant weld test of short transverse direction specimen, the fracture of welds shows lamellar tearing, which occurs in the heat affected zone so far  $100\mu$  from weld bond area. The fracture morphology shows intergranular fracture mainly, but microcracks by eutectic melting increased with increasing of weld heat input.

**KEY WORDS:** (Al Mg Alloy) (Heat Affected Zone) (Laminated Fracture) (Lamellar Tearing) (Fractography)

## 1. Introduction

Al-Mg series 5083 aluminum alloy has characterized by ease of welding, good strength and good toughness at low temperature.

Therefore, this alloy has been widely used for LNG tank and other cryogenic weldments. As the use of large weldments increases, thick plates above 50 mm and fillet welds are applied more. This alloy has rolling texture structure and highly directional grain boundaries by rolling process. Therefore, the mechanical strength of longitudinal (L) direction seems to be different from that of short transverse (ST) direction.

Generally, the fracture toughness and the stress corrosion cracking<sup>1)2)</sup> are considered to be affected by factors such as  $\beta$  phase ( $\text{Mg}_2\text{Al}_3$ ), inclusion, relatively insoluble compounds and shape of grain.

Recently, as the L direction specimen with notch was tensile-fractured at low temperature such as  $-196^{\circ}\text{C}$ , many subcracks perpendicular to the fracture surface occur, and which propagate parallel to the flat grain. Therefore, such a fracture morphology has been proposed as "laminated fracture". The mechanism has been proposed by many investigators<sup>3)4)</sup> but is not clearly explained yet. The other way, for fillet welds, to make

clear the fracture and the morphology of ST direction specimen is necessary to evaluate the actual fracture accident for cryogenic weldments. In the present investigation, the fracture phenomenon of ST direction specimen has been investigated, and the authors found that lamellar tearing occurs in 5083 aluminum alloy and its welds. Then, an investigation has been made into the effects of relatively insoluble compounds, inclusions, rolling texture structure and  $\beta$  phase precipitation on the lamellar tearing and laminated fracture at  $-196^{\circ}\text{C}$  by means of fractography.

## 2. Experimental Procedure

Chemical compositions of materials used are shown in Table 1. 5083 (A) material was mainly used to the

Table 1 Chemical compositions of materials used (wt%)

Materials	Cu	Si	Fe	Mn	Mg	Zn	Cr	Ti	Zr	Al	*	**
5083 (A)	0.02	0.15	0.20	0.64	4.7	0.01	0.11	0.01	-	Bal.	62 <sup>t</sup>	O
5083 (B)	0.02	0.15	0.21	0.64	4.7	0.01	0.10	0.02	-	Bal.	35 <sup>t</sup>	O
5183	0.04	0.06	0.07	0.71	5.16	<0.01	0.15	0.07	<0.01	Bal.	2 <sup>φ</sup>	-

\* Plate thickness or wire diameter

\*\* Heat treatment

† Received on September 17, 1979

\* Professor

\*\* Research Instructor

\*\*\* Graduate Student (Presently, Tokyo Shibaura Electric Co., Ltd.)

investigation of base metal and welds. Fig. 1 shows the specimen dimension for notch tensile test of base metal. Fig. 2 shows the specimen dimensions for implant weld test. Silicone oil bath and salt bath were used for heat treatment of base metal<sup>1)</sup>. The heat-treated specimens

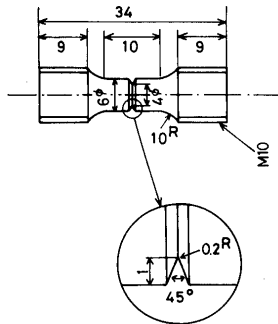


Fig. 1 Specimen dimension of base metal with V notch.

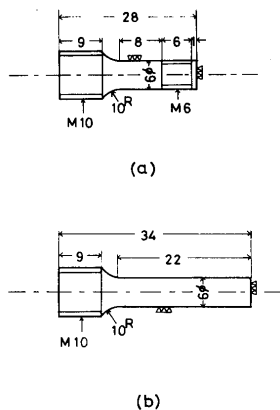


Fig. 2 Specimen dimensions of implant specimen for implant weld test. (a): with spiral notch, (b): without notch

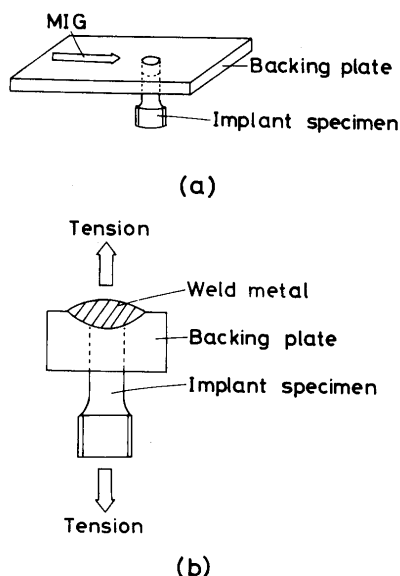


Fig. 3 Schematic diagram for implant weld test

were tensile-tested at  $-196^{\circ}\text{C}$  and then, the notch tensile strength (NTS) was evaluated. For the fracture test of welds, implant weld test was carried out in this investigation as shown in Fig. 3. As shown in Fig. 3-(a), the hole of 6 mm diameter was made in the backing plate, the implant specimen was inserted in the hole, and then MIG welding by DCSP was carried out on the plate. After welding, as shown in Fig. 3-(b), a block contained the implant specimen was cut off from the backing plate. The implant test specimen of the block was tensile-tested at  $-196^{\circ}\text{C}$  using Instron type tensile machine, and then the fracture stress of welds was evaluated. Well, 5083-O material of 10 mm thickness was used as the backing plate, the dimension was 200 (l)  $\times$  100 (w)  $\times$  10 (t). Weld filler metal was used 5183 alloy of 2 mm diameter. The fracture surface obtained was observed using scanning electron microscope.

### 3. Results and Discussions

#### 3.1. Effects of rolling texture structure and heat treatments on mechanical properties.

Fig. 4 shows the change in Charpy impact value at

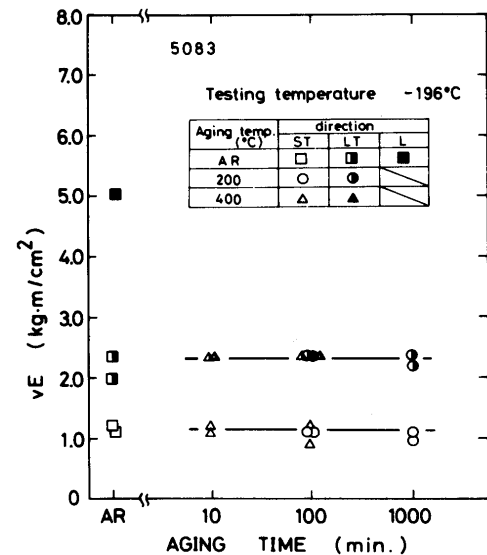


Fig. 4 Effects of rolling texture structure and heat treatments on Charpy impact value at  $-196^{\circ}\text{C}$

$-196^{\circ}\text{C}$  when L direction, LT (long transverse) direction and ST direction specimens were aged at various temperatures. Considering of the weld heat affected zone, the specimens were heat-treated at  $200^{\circ}\text{C}$  and  $400^{\circ}\text{C}$ . For  $400^{\circ}\text{C}$  heat treatment,  $\beta$  phase solutionizes completely and relatively insoluble compounds such as  $\text{Al}_{12}\text{Fe}_3\text{Si}$ ,  $\text{Al}(\text{Fe}, \text{Mn})\text{Si}$  precipitate more<sup>1)</sup>. For  $200^{\circ}\text{C}$  aging treatment,  $\beta$  phase precipitates in the grain and at the

grain boundary, though the relatively insoluble compounds hardly change<sup>1)</sup>.

The impact value of L direction specimen was 5 kg-m/cm<sup>2</sup>, the value of LT direction specimen was 2 kg-m/cm<sup>2</sup> and that of ST direction specimen was 1 kg-m/cm<sup>2</sup>. That of ST direction specimen is too low as well as that of low temperature brittleness of steels. Therefore, it is necessary to consider enough for the planning adopted the fillet welds. Well, Charpy impact value hardly depend on the relatively insoluble compounds and  $\beta$  phase precipitation for 400°C and 200°C heat treatments. It seems that the shape of grain, namely rolling texture structure has direct effects upon the impact value. Then, the effects of grain shape and heat treatment on notch tensile strength of L direction and ST direction specimens were investigated. The results are shown in Fig. 5. The chemical compositions of

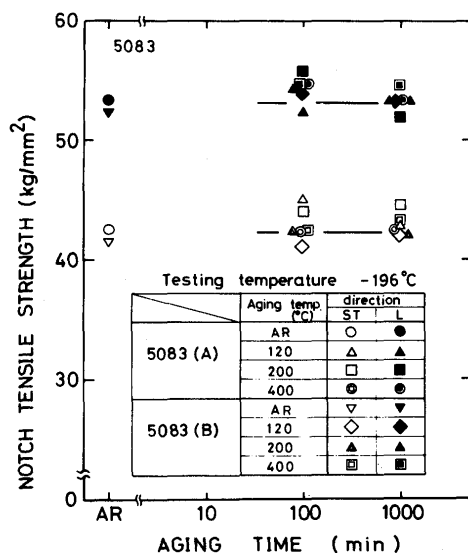


Fig. 5 Effects of rolling texture structure and heat treatments on notch tensile strength at  $-196^{\circ}\text{C}$ .

5083(A) material and 5083(B) material are almost same value as shown in Table 1.

The difference of these materials is plate thickness by difference of finishing rolling, and the degree of directional grain boundaries. The mean grain size of short axis for 5083(A) material was 14 microns and that for 5083(B) material was 8 microns.

For 120°C heat treatment,  $\beta$  phase precipitates at the grain boundary<sup>1)</sup>. The results show that the notch tensile strength is not affected very much by these heat treatments. The notch tensile strength of material used is hardly affected by grain shape in the range of this experiment, too. It seems that stress applied perpendicular to highly directional grain dominates the notch tensile strength at  $-196^{\circ}\text{C}$ .

### 3.2 Effects of recrystallization and grain boundary precipitates on notch tensile strength

As the alloy is aged at about 120°C,  $\beta$  phase precipitates at the grain boundary, and the susceptibility to stress corrosion cracking increases.<sup>1)2)</sup> Then, in this section, effects of  $\beta$  phase precipitation at the grain boundary, relatively insoluble compounds and recrystallization on the notch tensile strength at  $-196^{\circ}\text{C}$  were investigated. The results are shown in Fig. 6.

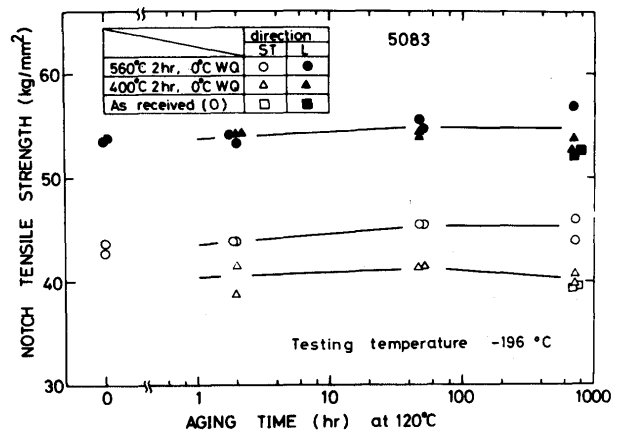


Fig. 6 Effects of recrystallization and grain boundary precipitates on notch tensile strength at  $-196^{\circ}\text{C}$ .

For 120°C aging treatment,  $\beta$  phase at the grain boundary increases with increasing of aging time, and as aging time becomes prolonged time,  $\beta$  phase at the grain boundary precipitates continuously. But as shown in Fig. 6,  $\beta$  phase precipitation has hardly effects upon the notch tensile strength at  $-196^{\circ}\text{C}$  in both L direction specimen and ST direction specimen. In this alloy, recrystallization hardly occurs for 400°C heat treatment, but partially occurs for 560°C heat treatment.<sup>1)</sup> For L direction specimen, the notch tensile strength is about 53 kg/mm<sup>2</sup> and is independent of the heat treatment in both 400°C and 560°C heat-treated specimens.

That is, the grain shape has not effects upon the notch tensile strength in spite of change of longitudinal axis of grain. For ST direction specimen, the grain shape changes with the difference of solution temperature, and then the notch tensile strength of 560°C heat-treated specimen is about 4 kg/mm<sup>2</sup> higher than that of 400°C heat-treated specimen. Well, the notch tensile strength of ST direction specimen is about 10 kg/mm<sup>2</sup> lower than that of L direction specimen. Therefore, the notch tensile strength of 5083 aluminum alloy is hardly affected by the grain boundary precipitates and the relatively insoluble compounds, but the grain shape and the direction of applied stress have effects on the notch tensile strength very much.

### 3.3 Effect of weld heat input on the fracture stress of welds

The notch tensile strength of ST direction specimen is lower than that of L direction specimen as shown in Fig. 5 and Fig. 6, therefore, for fillet welds, the fracture can be occurred in heat affected zone of base metal rather than in weld metal. Then, the effect of weld heat input on the fracture stress of implant test was investigated. The results are shown in Fig. 7. Well, the implant specimen is

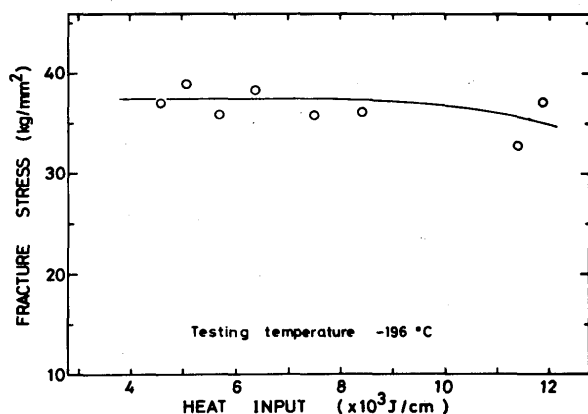


Fig. 7 Effect of weld heat input on fracture stress of welds by implant weld test.

ST direction specimen with spiral notch.

The fracture stress at  $-196^\circ\text{C}$  decreases slightly with increasing of weld heat input in the range of 12000 J/cm from 4000 J/cm. The fracture stress is lower than that of Fig. 6 for the reason of spiral notched specimen. The fracture position was heat affected zone of base metal.

### 3.4. Fractography on the lamellar tearing

#### 3.4.1 Effects of grain boundary precipitates on lamellar tearing and laminated fracture

Photo. 1 shows the fractographs of L direction and ST direction specimens for 5083-O material at  $-196^\circ\text{C}$ . All over the specimen of L direction is shown in Photo. 1-(a). Subcracks perpendicular to the main fracture surface are present stratifiedly. This fracture morphology is known as "laminated fracture". It seems that this phenomenon depends on the flat grain shape occurred by rolling process. Fracture morphology enlarged the subcrack is shown in Photo. 1-(b). Surface of subcrack is flat considerably and seems to have occurred the intergranular fracture. The area between subcracks shows fine dimple pattern and that is transgranular fracture. Massive inclusion and relatively insoluble compounds are present a

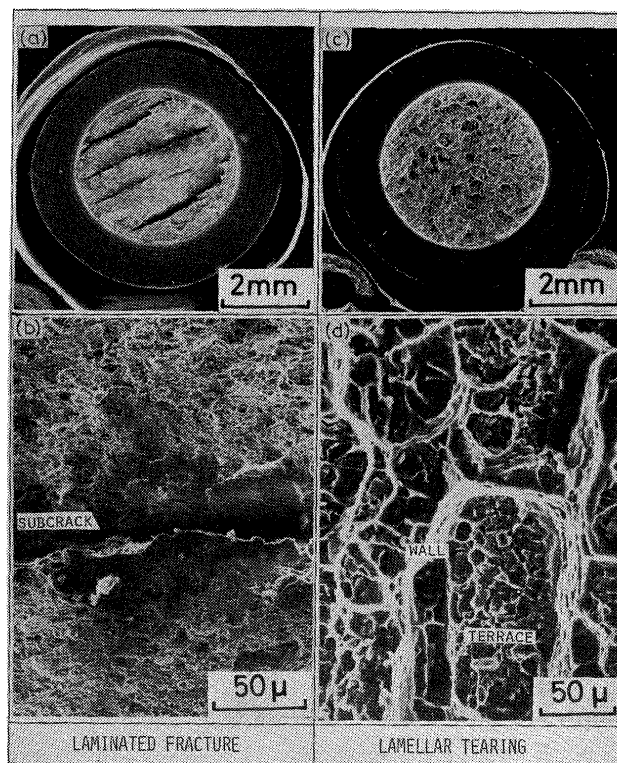
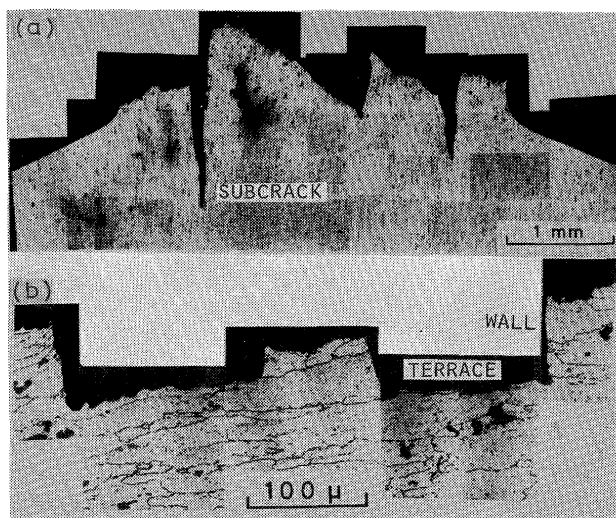


Photo. 1 Fractographs of L direction and ST direction specimens of 5083-O material at  $-196^\circ\text{C}$ . (a): Macro appearance showing laminated fracture, (b): Subcracks along the grain boundary, (c): Macro appearance of lamellar tearing showing terrace and wall, (d): Inclusions and relatively insoluble compounds on the terrace area.

few on the dimple bottom. By means of X-ray spot analysis of energy dispersion method, the inclusions was Al (Fe,Mn). All over the ST direction specimen is shown in Photo. 1-(c). Subcrack was hardly recognized on the fracture surface on the contrary to L direction specimen. As shown in Photo. 1-(d), dark areas are recognized, the area is surrounded by the white band, and then inclusions are distributed widely on the plane in the dark area. This area is proposed as "terrace" by Elliot.<sup>6)</sup> The white band connected with the terrace area is proposed as "wall", and shows shear dimple. We proposed as "lamellar tearing" the terrace and wall type fracture in the case of aluminum alloy as well as that of steels.<sup>7)</sup> The area between inclusions and relatively insoluble compounds on the terrace area showed fine dimple pattern or tear ridge.

According to Photo. 1-(d) enlarged the terrace area, flat inclusions and relatively insoluble compounds are present on the dimple bottom, and they are cubic<sup>1)</sup> and showed cleavage fracture at  $-196^\circ\text{C}$ . Consequently, fracture morphology of ST direction specimen of 5083-O material at  $-196^\circ\text{C}$  was transgranular fracture with terrace and wall, namely lamellar tearing.

Photo. 2 shows the microstructures showing crack



**Photo. 2** Microstructures showing crack profile of 5083-O material at  $-196^{\circ}\text{C}$ . (a): Laminated fracture in L direction specimen, (b): Lamellar tearing in ST direction specimen

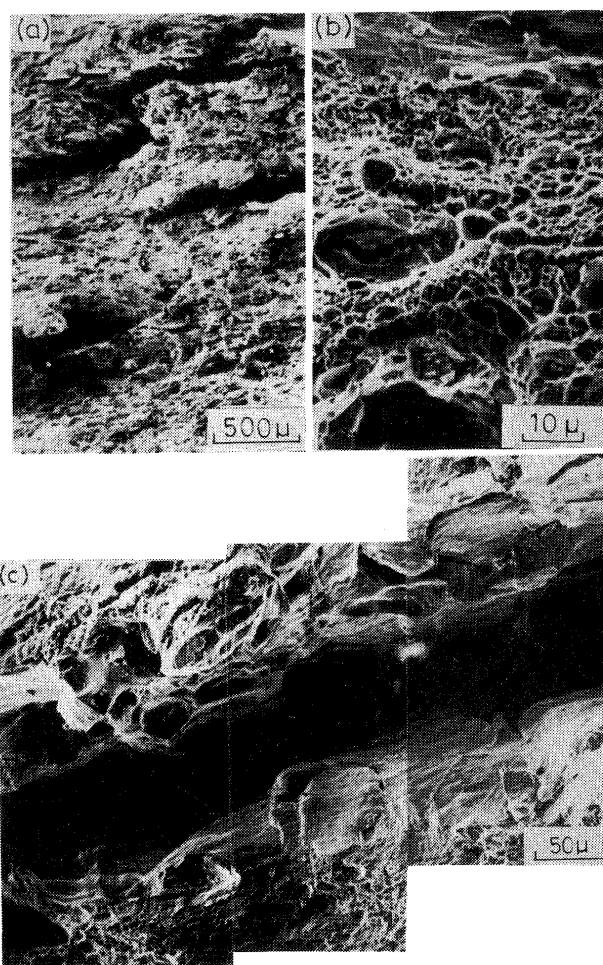
profile of L direction specimen and ST direction specimen at  $-196^{\circ}\text{C}$  test.

Photo. 2-(a) shows the laminated fracture in L direction specimen. Subcracks perpendicular to main cracks were recognized and the depth was  $500\mu$  to  $1500\mu$ . For the main crack, the fracture proceeded with shear type. Well, the subcrack was hardly recognized at  $25^{\circ}\text{C}$  test. Photo. 2-(b) shows the lamellar tearing in ST direction specimen. The fracture profile shows terrace and wall type. The terrace area is parallel to the flat grain, and it looks like intergranular fracture.

But on the basis of the detail observation, the terrace area shows transgranular fracture. That is, the inclusions are distributed flat and laminated in the flat grain by rolling process. The interface of inclusion and matrix, or inclusions themselves seems to be origin position of the fracture. The wall area is flat at  $-196^{\circ}\text{C}$ , but at  $25^{\circ}\text{C}$ , the wall area was deformed and not flat. Namely, at room temperature fracture, lamellar tearing was not clearly recognized for the reason of deformation.

**Photo. 3** shows the fractographs of laminated fracture at  $-196^{\circ}\text{C}$  for L direction specimen solutionized at  $560^{\circ}\text{C}$  for 2 hours, and then aged at  $120^{\circ}\text{C}$  for 1 month. As shown in Photo. 3-(a), subcracks are present stratifiedly on the fracture surface.

The area between subcracks is shown in Photo. 3-(b) and is main crack area. The fracture morphology shows transgranular fracture showing dimple pattern. The photograph enlarged near the subcrack is shown in Photo. 3-(c). For  $560^{\circ}\text{C}$  solution heat treatment, the relatively insoluble compounds are solutionized considerably and recrystallization occurs, and for  $120^{\circ}\text{C}$  1 month aging,  $\beta$



**Photo. 3** Fractographs at  $-196^{\circ}\text{C}$  for L direction specimen heat-treated at  $560^{\circ}\text{C}$  for 2 hours and then aged at  $120^{\circ}\text{C}$  for 1 month. (a): Fractograph showing laminated fracture, (b): Main crack showing dimple pattern with inclusion, (c): Subcrack showing intergranular fracture in recrystallization structure

phase precipitates at the grain boundary continuously.<sup>1)</sup>

Therefore, the characteristic by the treatment seems to be shown on the fracture morphology, generally. The area of subcrack shows intergranular fracture and the subcrack occurred along the grain boundary in recrystallization structure. Slide lines occurred by plastic deformation were recognized on the intergranular fracture surface. The subcrack is considered to have occurred formerly rather than occurrence of main crack.

Circumference area of the subcrack shows dimple pattern, and is transgranular fracture. Consequently, the main crack for L direction specimen is transgranular fracture, not depends on the grain boundary precipitates but depends on the inclusions and the relatively insoluble compounds. **Photo. 4** shows the fractographs of laminated fracture at  $-196^{\circ}\text{C}$  for L direction specimen heat-treated at  $400^{\circ}\text{C}$  for 2 hours, and then aged at  $120^{\circ}\text{C}$

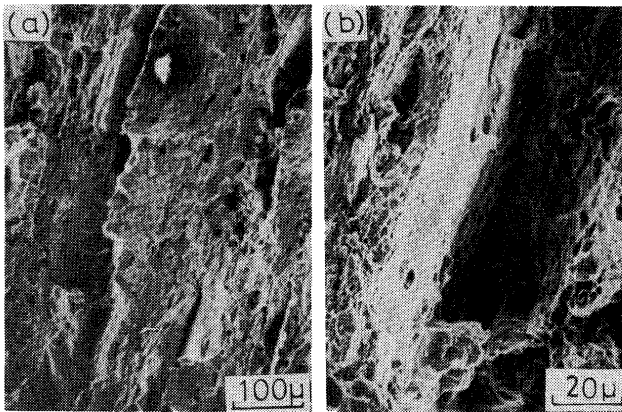


**Photo. 4** Fractographs at  $-196^{\circ}\text{C}$  for L direction specimen heat-treated at  $400^{\circ}\text{C}$  for 2 hours and then aged at  $120^{\circ}\text{C}$  for 1 month. (a): Fractograph showing laminated fracture, (b): Subcrack showing intergranular fracture in nonrecrystallization structure.

for 1 month. For  $400^{\circ}\text{C}$  heat treatment, the relatively insoluble compounds precipitate more, but recrystallization hardly occurs on the contrary to  $560^{\circ}\text{C}$  heat treatment.<sup>1)</sup>

And the grain shape is flat as well as as-received material (O). Photo. 4-(a) shows the laminated fracture with subcracks. The subcracks are present stratifiedly on the fracture surface, and show flat intergranular fracture as shown in Photo. 4-(b).

The morphology of subcrack is same as that of as-received material shown in Photo. 1-(b). **Photo. 5** and **Photo. 6** show the fractographs of lamellar tearing at  $-196^{\circ}\text{C}$  for ST direction specimens heat-treated at  $560^{\circ}\text{C}$  or  $400^{\circ}\text{C}$  for 2 hours respectively and then aged at  $120^{\circ}\text{C}$  for 1 month. For  $560^{\circ}\text{C}$  heat-treated specimen, as shown

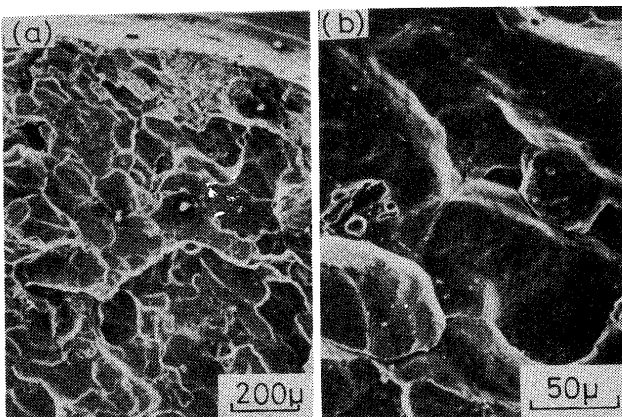


**Photo. 5** Fractographs at  $-196^{\circ}\text{C}$  for ST direction specimen heat-treated at  $560^{\circ}\text{C}$  for 2 hours and then aged at  $120^{\circ}\text{C}$  for 1 month. (a): Fractograph showing lamellar tearing, (b): Main crack showing flat intergranular fracture in the recrystallization structure, subcrack is hardly present.

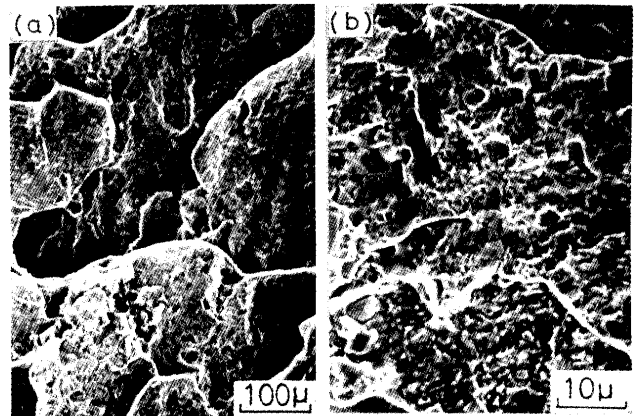


**Photo. 6** Fractographs at  $-196^{\circ}\text{C}$  for ST direction specimen heat-treated at  $400^{\circ}\text{C}$  for 2 hours and then aged at  $120^{\circ}\text{C}$  for 1 month. (a): Fractograph showing lamellar tearing, (b): Main crack showing uneven intergranular fracture in the nonrecrystallization structure.

in Photo. 5-(a), the grain size is small for the reason of recrystallization. The fracture morphology shows flat intergranular fracture as shown in Photo. 5-(b). Therefore, the lamellar tearing shows intergranular fracture for the reason of  $\beta$  phase precipitated at the grain boundary continuously.

The other way, for  $400^{\circ}\text{C}$  heat-treated specimen as shown in Photo. 6, the fracture morphology of lamellar tearing shows uneven intergranular fracture, and on the fracture surface, inclusions and relatively insoluble compounds are present a few.

Precipitation behavior of  $\beta$  phase at  $120^{\circ}\text{C}$  can be affected by the solution temperature. Therefore, the difference of  $560^{\circ}\text{C}$  heat treatment and  $400^{\circ}\text{C}$  heat treatment seems to have been appeared on the fracture morphology. The recrystallization hardly occurs for  $400^{\circ}\text{C}$  heat treatment, and both transgranular fracture and intergranular fracture are shown as the lamellar tearing. The fracture type can be distinguished only fractography. Well, as  $\beta$  phase precipitates at the grain boundary, the mechanical strength hardly changes as shown in Fig. 6, but the fracture morphology of lamellar tearing for ST direction specimen changes from transgranular fracture to intergranular fracture.

Generally, investigations on the laminated fracture have been widely made. Sawkill<sup>3)</sup> explained the phenomenon by the reason that the mechanical property of ST direction is lower than that of L direction. Lismer<sup>5)</sup>, Asano<sup>8)</sup> etc, considered that the subcrack occurred by lowering of bonding force at the grain boundary. The other way, Ikeda<sup>4)</sup> considered that inclusions and relatively insoluble compounds contained manganese and chromium are present parallel to rolling



structure, and the laminated fracture occurred at the interface between them and matrix. In the present investigation, it is concluded that the laminated fracture, namely the subcracks occurred along the grain boundaries, but hardly occurred at the inclusions and relatively insoluble compounds. Therefore, the laminated fracture was considered to be occurred not only by lowering of bonding force at the grain boundary but also by the mechanic's factor based on the material anisotropy by the flat grain shape. That is, it is considered that local stress concentration and deformation occurred at the grain boundary, as the result, subcrack occurred along the grain boundary. The other way, the fracture morphology of ST direction specimen showed lamellar tearing of terrace and wall type. As  $\beta$  phase precipitates at the grain boundary a few or few, the lamellar tearing occurs at the interface between inclusion and relatively insoluble compounds, and the matrix. As  $\beta$  phase precipitates at the grain boundary continuously, the lamellar tearing occurs at the grain boundary. Consequently, lamellar tearing is considered to occur by materials's factor rather than by mechanic's factor such as laminated fracture.

### 3.4.2 Fractography of welds by implant test

In the present investigation, implant weld test was carried out in order to investigate the lamellar tearing of 5083 aluminum alloy welds. One of the results is shown in **Photo. 7**.

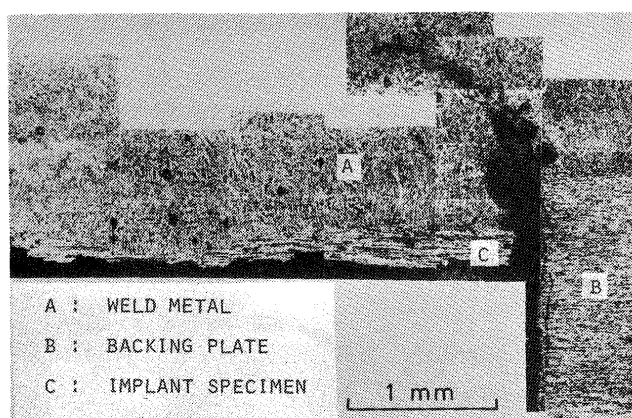


**Photo. 7** Microstructure showing lamellar tearing in the implant weld test.

Implant specimen is ST direction specimen without notch.

Mark A is weld metal, Mark B is backing plate and Mark C is fracture area of the implant specimen. One of cracks propagates toward the weld metal and stopps, but main crack propagates in the heat affected zone in the range of  $100\mu$  so far from bond area of the implant

specimen. The crack profile shows lamellar tearing of terrace and wall type. Well, for the implant specimen of L direction, the fracture occurred in the weld metal.

Therefore, the fracture stress of ST direction implant specimen seems to be lower than that of weld metal and L direction implant specimen, and the lamellar tearing of actual weldments will occur at the fillet welds, not in the butt welds.

**Photo. 8** shows the fractographs of the implant

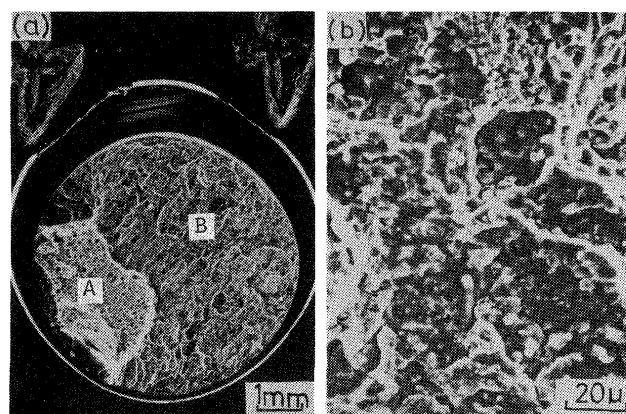


**Photo. 8** Fractographs at  $-196^{\circ}\text{C}$  for implant ST direction specimen without notch. (a): Macro appearance showing lamellar tearing, (b): Fractograph in heat affected zone

specimen side of **Photo. 7**. **Photo. 8**-(a) shows the whole aspects. Mark A is weld metal and Mark B is heat affected zone of base metal. In the heat affected zone, the fracture morphology shows lamellar tearing of terrace and wall. **Photo. 8**-(b) shows the fractograph enlarged the heat affected zone, the fracture morphology shows microcrack by eutectic melting<sup>9)</sup> at the grain boundary, and the fracture area seems to be the area heated above  $560^{\circ}\text{C}$  in the vicinity of weld bond area. **Photo. 9** shows the fractographs at  $-196^{\circ}\text{C}$  for implant test specimen. Weld heat input was  $11900 \text{ J/cm}$ . Well, the implant specimen is ST direction specimen with spiral notch. Lamellar tearing of terrace and wall type occurred as shown in **Photo. 9**-(a). The fracture position was the heat affected zone of base metal. Enlarging **Photo. 9**-(a), the fracture morphologies of two types were recognized, namely intergranular fracture shown in **Photo. 9**-(b) and **Photo. 9**-(c), and microcrack by eutectic melting shown in **Photo. 9**-(d) were observed. On the basis of the ratio of fracture morphology, the area of microcrack distributed more than that of intergranular fracture. Therefore, the lamellar tearing of this heat input considered to have occurred at the area heated above  $560^{\circ}\text{C}$  near the bond area. **Photo. 10** shows the fractographs at  $-196^{\circ}\text{C}$  for implant test specimen. The implant specimen is ST



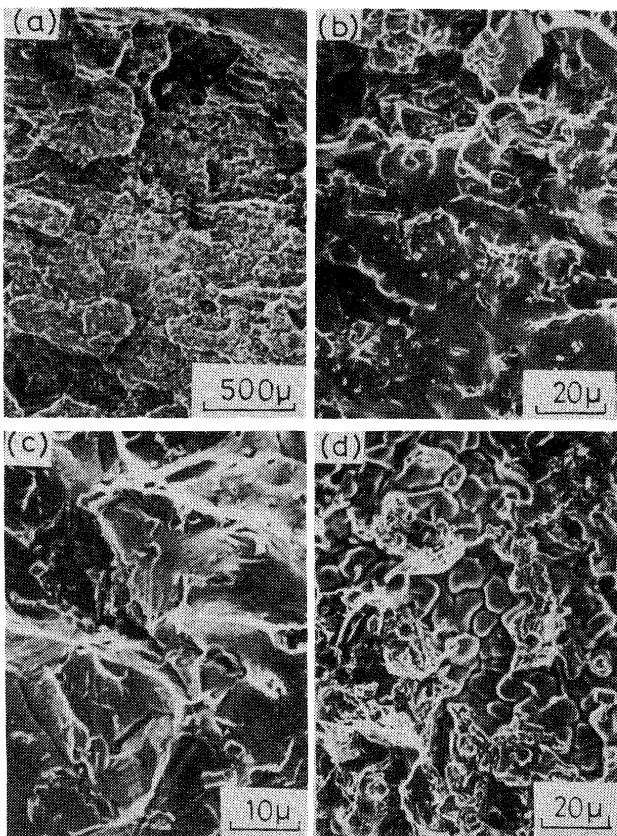


**Photo. 9.** Fractographs of lamellar tearing at  $-196^{\circ}\text{C}$  for implant ST direction specimen with spiral notch. (11900 J/cm) (a): Fractograph showing lamellar tearing, (b): Intergranular fracture in recrystallization structure, (c): Fracture along grain boundary, (d): Micro crack occluded by eutectic melting.

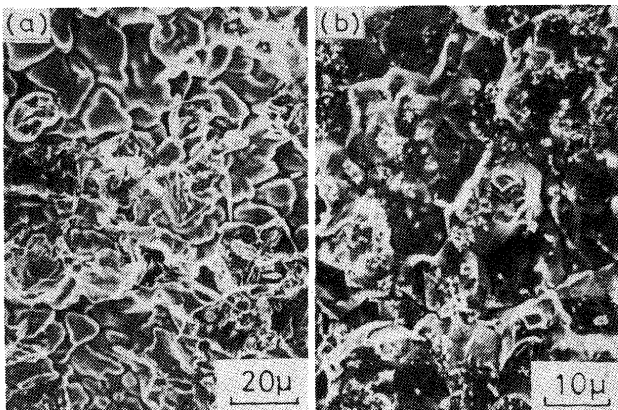


**Photo. 10** Fractographs of lamellar tearing at  $-196^{\circ}\text{C}$  for implant ST direction specimen with spiral notch. (7500 J/cm) (a): Microcrack occurred by eutectic melting, (b): Intergranular fracture in recrystallization structure.

direction specimen with spiral notch. Weld heat input was 7500 J/cm.

Both microcrack by eutectic melting shown in Photo.

10-(a) and intergranular fracture in recrystallization structure shown in Photo. 10-(b) were recognized. The fracture position seems to be the heat affected zone heated up to  $600^{\circ}\text{C}$  from  $560^{\circ}\text{C}$ .

**Photo. 11** shows the fractographs at  $-196^{\circ}\text{C}$  for

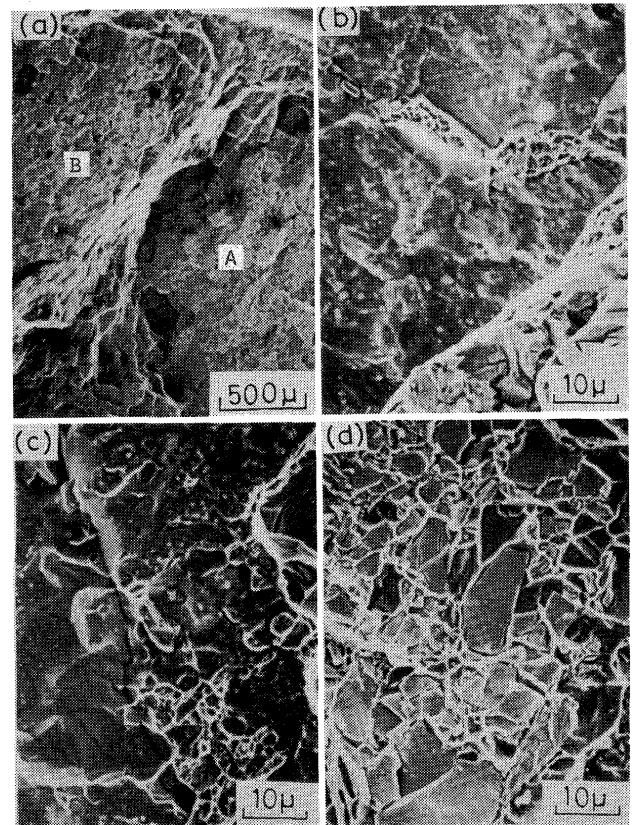


**Photo. 11** Fractographs of lamellar tearing at  $-196^{\circ}\text{C}$  for implant ST direction specimen with spiral notch. (4600 J/cm) (a): Fractograph showing lamellar tearing, (b): intergranular fracture in non-recrystallization structure in Mark A, (C): Intergranular fracture in recrystallization structure in Mark A, (d): Transgranular fracture with inclusions and relatively insoluble compounds in terrace area in Mark B.

implant test specimen. Weld heat input was 4600 J/cm. Implant specimen is ST direction specimen with spiral notch. As shown in Photo. 11-(a), the fracture morphology shows lamellar tearing of large terrace and wall type.

Mark A is the heat affected zone near the bond area. The fracture morphology in Mark A area shows intergranular fracture in both nonrecrystallization structure shown in Photo. 11-(b) and recrystallization structure shown in Photo. 11-(c). In the area of Mark B of Photo. 11-(a), many flat inclusions and relatively insoluble compounds are present on the terrace area, and which showed cleavage fracture by cubic as shown in

Photo. 11-(d).

In the heat input of 4000 J/cm to 12000 J/cm, the fracture position of lamellar tearing is affected by the weld heat input.

Namely, when weld heat input is low, the fracture position is the heat affected zone of recrystallization structure and the fracture morphology shows intergranular fracture, or the area of nonrecrystallization structure heated up to 500°C and the fracture morphology is dimple pattern with flat inclusions and relatively insoluble compounds. When the weld heat input is high, the fracture position is the heat affected zone. The fracture morphology shows intergranular fracture in the recrystallization structure or microcrack by eutectic melting.

The area seems to have been heated above 560°C. The microcrack increases with increasing of weld heat input. Consequently, on the larger weld heat input, the phenomenon is very important.

And it seems that fracture stress of welds decreases with increasing of weld heat input.

#### 4. Conclusion

An investigation has been made into the lamellar tearing of 5083 aluminum alloy and its welds at -196°C by means of fractography. The results obtained in this investigation are summarized as follows.

- (1) Charpy impact value and notch tensile strength at -196°C becomes lower in the order of L direction, LT direction and ST direction, for the reason that the alloy has rolling texture structure and highly directional grain boundaries.
- (2) The relatively insoluble compounds and  $\beta$  phase have hardly effects on the impact value and the notch tensile strength at -196°C.
- (3) For L direction specimen, laminated fracture with many subcracks occurs independent of  $\beta$  phase precipitation at the grain boundary. Subcracks occur along the flat grain boundary by rolling process, and main crack is transgranular fracture independent of  $\beta$  phase at the grain boundary.
- (4) For ST direction specimen, "lamellar tearing" occurs, which shows terrace and wall type fracture. As  $\beta$  phase hardly precipitates, the fracture morphology shows transgranular fracture, and relatively insoluble

compounds and inclusions are present in the terrace area. When  $\beta$  phase precipitates at the grain boundary continuously, the fracture morphology shows intergranular fracture. In the case of non-recrystallization structure, lamellar tearing of terrace and wall type occurs in spite of intergranular fracture.

- (5) For implant weld test of ST direction specimen, the fracture stress of welds slightly decreases with increasing of weld heat input.
- (6) The fracture morphology of welds shows lamellar tearing, and the crack propagates in the heat affected zone so far 100 microns from weld bond area. Intergranular fracture mainly occurred in the recrystallization structure heated above 500°C. But microcrack by eutectic melting increases with increasing of weld heat input.

For large heat input welding, microcrack increases, and fracture stress of welds seems to decrease.

#### Acknowledgements

The authors wish to thank Mr. T. Horinouchi for his variable contribution in this work. The support of the Light Metal Educational Foundation is gratefully acknowledged.

#### References

- 1) T. Enjo, T. Kuroda and H. Shinonaga: Effect of relatively insoluble compounds on  $\beta$  phase precipitation in 5083 aluminum alloy, Trans. JWRI, 7, (1978), 173
- 2) T. Enjo, T. Kuroda and H. Shinonaga: Effects of relatively insoluble compounds and  $\beta$  phase on stress corrosion cracking in 5083 aluminum alloy, Trans. JWRI, 8, (1979), 67
- 3) J. Sawkill and D. James, British Weld. J., 11 (1958), 517
- 4) T. Ikeda et., J. Japan Inst. of Light Metals, 23, (1973), 393
- 5) E. Lismer, British Weld. J. 11, (1958) 523
- 6) D. N. Elliott: A fractographical examination of lamellar tearing in multi run fillet welds, Metal Construction and British Weld. J., 2, (1969), 50
- 7) T. Kuroda: Hydrogen embrittlement and its fractography in high tensile strength steel and its welds, Doctor Thesis, (Osaka University), (1976), P 108 (In Japanese)
- 8) K. Asano and A. Fujiwara: Laminated fracture of 5083 alloy at low temperature, J. Japan Inst. of Light Metals, 26, (1976), 27 (In Japanese)
- 9) T. Arita et al.: Studies on micro-cracks in 5083 aluminum alloy thick plate welds, J. of Light Metal Welding and Constructions, 14, (1976), 305 (In Japanese)